ANTIOXIDANTS & REDOX SIGNALING
Volume 22, Number 9, 2015

DOI: 10.1089/ars.2014.5963

Discoveries

ORIGINAL RESEARCH COMMUNICATION

HYPERSENSITIVE RESPONSE-LIKE LESIONS 1 Codes for AtPPT1 and Regulates Accumulation of ROS and Defense Against Bacterial Pathogen *Pseudomonas syringae* in *Arabidopsis thaliana*

Aditya Dutta,* Samuel H.P. Chan, Noel T. Pauli,† and Ramesh Raina

Abstract

Aims: Plants employ both basal and resistance gene (*R* gene)-mediated defenses in response to pathogens. Reactive oxygen species (ROS) are widely reported to play a central role in both basal and *R* gene-mediated defense; however, the nature of ROS has been less well established for basal defense. In addition, spatial distribution of redox moieties and mechanisms of plant responses during basal defense are poorly understood. We investigated redox signaling in *Arabidopsis thaliana* in response to virulent bacterial pathogen, focusing on the role of the mitochondria in balancing energy demands against generation of physiologically relevant ROS. ***Results:*** Positional cloning of an *Arabidopsis* lesion mimic mutant identified a polyprenyl transferase involved in the biosynthesis of Coenzyme Q_{10} (CoQ), which leads to novel insights into physiological ROS levels and their role in basal resistance. Gain- and loss-of-function studies identified Coenzyme Q_{10} redox state to be a key determinant of ROS levels. These Coenzyme Q_{10} redox state-mediated ROS levels had a direct bearing on both response against pathogen and ability to thrive in high oxidative stress environments. ***Innovation:*** We demonstrate that Coenzyme Q_{10} redox state generates an ROS threshold for a successful basal resistance response. Perturbation of the Coenzyme Q_{10} redox state has the potential to disrupt plant defense responses against bacterial pathogens. ***Conclusions:*** Coenzyme Q_{10} redox state is a key regulator of *Arabidopsis* basal resistance against bacterial pathogens. *Antioxid. Redox Signal*. 22, 785–796.

Introduction

PLANTS EMPLOY BOTH BASAL and *R* gene-mediated defenses in response to pathogens (24). Basal defenses typically involve the detection of a pathogen-associated molecular pattern (PAMP), which includes flagellin, lipopolysaccharide, chitin, and other surface molecules that are common across a wide range of pathogens. Immunity in response to PAMPs is termed PAMP triggered immunity (PTI). However, pathogens suppress PTI by injecting effectors (also called virulence factors) into the plant cell. Plants recognize these effectors *via* receptor resistance proteins (a product of *R* genes) and mount effector-triggered immunity (ETI). Although both PTI and ETI help in suppressing the growth of

Innovation

Our study demonstrates that the redox status of Coenzyme Q_{10} is a key regulator of physiological reactive oxygen species (ROS) levels, which play a critical role in regulating basal resistance against bacterial pathogens in *Arabidopsis*. Our data suggest that perturbations of the Coenzyme Q_{10} oxidation state have a direct bearing on the redox status of the cell. Such redox changes alter appropriate orchestration of plant defense responses. We conclude that ROS generated as a result of basal cellular metabolic activities plays a critical role in maintaining basal resistance against bacterial pathogens in *Arabidopsis*.

Department of Biology, Syracuse University, Syracuse, New York.
*Current affiliation: Herbert Irving Comprehensive Cancer Center, Columbia University, New York, New York.
†Current affiliation: Department of Medicine, University of Chicago, Chicago, Illinois.

pathogens, PTI is unable to mount a successful defense response to clear out the pathogen. However, ETI, which is characterized by the hypersensitive response (HR) that leads to localized cell death at the point of infection and heightened resistance against secondary infection, is able to mount a successful defense against invading pathogens (24).

Signaling during both PTI and ETI is mediated *via* reactive oxygen species (ROS) (16). The rapid and transient induction of ROS (oxidative burst) is a defining hallmark of identification and subsequent defense activation against pathogens (28, 45). This induction of ROS is biphasic in nature and involves a first burst correlating to identification of the pathogen followed by a more intense and longer second burst, which correlates with activation of the plant defense response (20). ROS production in plants has been reported upon interaction with bacteria, fungi, viruses, insects, and nematodes (12, 14, 15, 25, 32), indicating that ROS production in response to pathogens is a central theme in activating plant defense networks. Prominent ROS involved in plant defense include hydrogen peroxide and superoxide that are distributed across different pools in the cell. ROS are generated either in response to external elicitation (for example, interaction with pathogen) or as a product of metabolic processes in the cell (for example, the electron transport chain in the mitochondria and chloroplast) (33, 46). Interplay between different ROS pools may modulate different responses and the intensity of these responses. ROS have been postulated to play multiple roles in its action against pathogens. These roles range from directly killing the pathogen (6), creating barrier structures by cross-linking cell wall glycoproteins (3), acting as signaling molecules (27), mediating generation of phytoalexins (44), and acting as a source for activation of further defenses (35). Interestingly, mitochondrial Complex II has been identified to play a key role in mitochondrial-derived ROS that affects gene regulation in both pathogen defense and stress responses (19).

In animal systems, mitochondria are a major source of generation of cellular ROS under steady-state conditions. However, in plants, mitochondria have been reported to diminish ROS production because of the presence of alternative oxidases (40, 47). Although alternative oxidases limit ROS production by keeping the electron transport chain oxidized, the exact magnitude of reduction of ROS in plant mitochondria relative to animal mitochondria has not been very well defined. However, plant mitochondria generate superoxide and hydrogen peroxide (the two major ROS) at rates comparable to animal mitochondria, not only on an absolute basis but also as a percentage of the rate of electron transport (34). Thus, mitochondrial electron transport chain-generated ROS are probably a major contributor to cellular ROS levels under normal physiological conditions.

Here, we present evidence that the redox state of Coenzyme Q_{10}, a component of the electron transport chain, is an important contributor to cellular ROS levels that modulate basal resistance of *Arabidopsis* against bacterial pathogens. We demonstrate that changes in the redox state of Coenzyme Q_{10} generate a ROS threshold for a successful basal resistance response. Thus, perturbation of the Coenzyme Q_{10} redox state has the potential to alter plant defense responses against bacterial pathogen. To that effect, we have characterized the role of HRL1, a polyprenyl transferase and a key enzyme involved in Coenzyme Q_{10} (CoQ) biosynthesis, in regulating defense against bacterial pathogen *Pseudomonas syringae*. An ethyl methanesulfonate (EMS)-generated *hrl1* (*hypersensitive response-like lesions 1*) mutant has been shown to suppress pathogen growth and has high levels of ROS (11). Overexpression of *HRL1* makes plants susceptible to the bacterial pathogen *P. syringae*. Furthermore, altering the levels of HRL1 in *HRL1* overexpressing and *hrl1* mutant plants positively and negatively affects production of Coenzyme Q_{10} (CoQ), an electron carrier in the mitochondrial electron transport chain. Modulation in *HRL1* also affects levels of reduced Coenzyme Q_{10} (ubiquinol), oxidized Coenzyme Q_{10} (ubiquinone), Coenzyme Q_{10} (CoQ) redox ratio (ubiquinol/ubiquinone), and total CoQ_{10}. In addition, *HRL1* overexpressing plants are also more resistant to high ROS environments. These results demonstrate that changes in the redox state of Coenzyme Q_{10} play a critical role in regulating basal resistance against *P. syringae* and ROS-mediated stress in *Arabidopsis.*

Results

Positional cloning of HRL1

The *hrl1* mutant was identified in an EMS-mutagenesis screen as a mutant that spontaneously developed HR-like lesions and had enhanced resistance against bacterial pathogens (11). *HRL1* was previously mapped to the lower arm of the fourth chromosome (11). Map-based cloning analysis was employed to identify and clone *HRL1*, which further allowed characterization of the role of HRL1 in defense signaling. *hrl1* mutant females (Col-0 ecotype) were crossed to L*er*-0 male (Landsberg *erecta* ecotype) wild-type plants, and CAPS markers (26) were used to analyze 960 F_2 progeny displaying the *hrl1* lesion-mimic phenotype. *HRL1* was found to be located between genetic markers SM90_137,6 and MI422 (Fig. 1 and Supplementary Table S1; Supplementary Data are available online at www.liebertpub.com/ars), which helped identify a 34 kb fragment (containing 13 genes in the F9D16 BAC) that was used for complementation analysis of the *hrl1* mutant. Complementation using overlapping fragments from

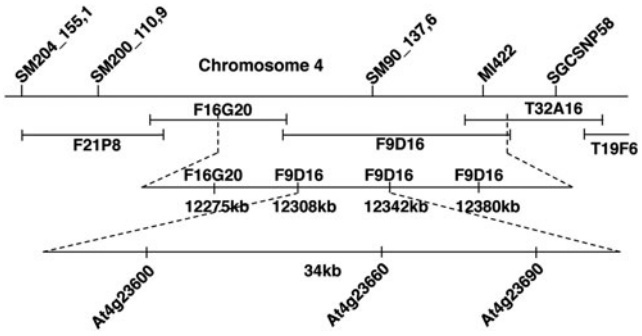

FIG. 1. Positional cloning of the *HRL1* gene. Diagram representing the *HRL1* region of *Arabidopsis* after mapping using CAPS markers. Single nucleotide polymorphisms and Insertion Deletions (InDels) were utilized to narrow down the *HRL1* genetic region to a smaller part of the lower arm of the fourth chromosome. The identified 34 kb region in BAC F9D16 was then digested into overlapping fragments, and complementation analysis was performed. Genetic markers covering the *HRL1* locus on the lower arm of chromosome 4 are indicated. *Arabidopsis* BAC clones around the *HRL1* region are indicated.

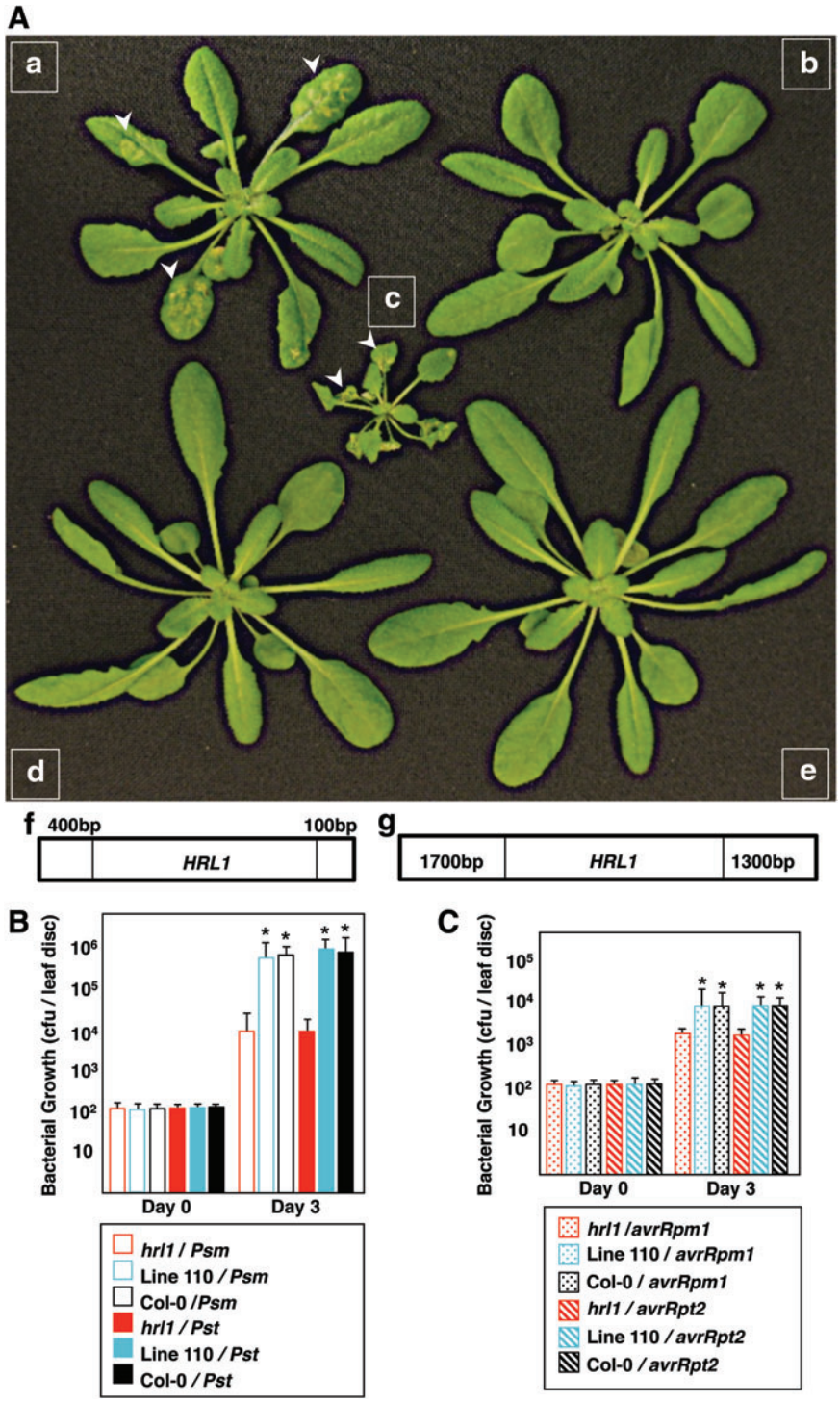

FIG. 2. Complementation of the *hrl1* mutant phenotype. **(A)** Phenotype of line 84 at 5 weeks **(a)**, line 84 at 3 weeks **(b)**, 5-week-old *hrl1* mutant **(c)**, 5-week-old line 110 **(d)** and 5-week-old wild-type Col-0 **(e)**, genomic fragment used for complementation in line 84 **(f)**, genomic fragment used for complementation in line 110 **(g)**. *Arrows* indicate lesions. **(B)** Rosette leaves of 4-week-old plants were infiltrated with virulent *Psm* ES4326 (*Psm*) and *Pst* DC3000 (*Pst)* at a titer of 5×10^5 cfu/ml. For each genotype, nine plants were tested individually. Two leaf discs from each plant were collected at day 0 and 3 dpi (days post infiltration). Bacterial growth is presented as cfu/leaf disc and represents the mean and SD of nine independent plants. The entire experiment was repeated at least twice more with plants grown at different times, and similar results were obtained. *Asterisks* indicate statistically significant differences ($*p < 0.001$, Mann–Whitney test). **(C)** Rosette leaves of 4-week-old plants were infiltrated with avirulent *Pst* DC3000 (*avrRpm1*) and *Pst* DC3000 (*avrRpt2*) at a titer of 5×10^5 cfu/ml. For each genotype, nine plants were tested individually. Two leaf discs from each plant were collected at day 0 and 3 dpi. Bacterial growth is presented as cfu/leaf disc and represents the mean and SD of nine individual plants. The entire experiment was repeated at least twice more with plants grown at different times, and similar results were obtained. *Asterisks* indicate statistically significant differences ($*p < 0.001$, Mann–Whitney test). To see this illustration in color, the reader is referred to the web version of this article at www.liebertpub.com/ars

F9D16 was carried out using partially digested Sau3AI fragments of F9D16 BAC cloned into the binary vector pYLTAC7 (obtained from ABRC) and subsequently transformed into the *hrl1* mutant. Screening for complementation of the *hrl1* phenotype identified a single line (line 84) that successfully complemented the *hrl1* phenotype of small size and lesion formation early in development (3 weeks postgermination). However, spontaneous lesions developed later in development (5 weeks) (Fig. 2A). To identify the F9D16 fragment responsible for the partial rescue of phenotype, sequencing of the engineered clone was carried out, which identified a fragment spanning a single gene At4g23660 (Fig. 2A) along with its flanking regions (total of 4.5 kb). A larger fragment containing At4g23660 and additional flanking regions that included a complete promoter was cloned from F9D16 (total of 7 kb) (Fig. 2A). This fragment was able to fully complement the *hrl1* mutation (line 110). Line 110 did not develop any lesions, and its size was also restored to that of the wild-type Col-0 plants (Fig. 2A). Furthermore, constitutive defense gene expression and defense against pathogens (both of which are hallmarks of the *hrl1* lesion-mimic mutant) in this line were suppressed to levels similar to those of the wild-type Col-0 plants (Fig. 2B, C and Supplementary Fig. S1A–C). Taken together, these results demonstrate that the insert in line 110, which contains the At4g23660 gene along with its 5′ and 3′ regulatory sequences, is able to fully complement the *hrl1* mutation.

Single amino-acid change is responsible for hrl1 *mutant phenotype*

At4g23660 is annotated to code for a polyprenyl transferase involved in the biosynthesis of Coenzyme Q_{10} (CoQ), an electron carrier in the electron transport chain (37). The 4 kb *HRL1* genomic fragment along with 1.7 kb upstream and 1.3 kb downstream regions were completely sequenced to identify mutation(s) responsible for the *hrl1* lesion-mimic phenotype (11). No mutations were found in either the upstream or downstream flanking regions. However, a single base change in an exon, which substituted a cytosine for a thymine, was identified at position 682 in the coding sequence. Sequencing of the complementary DNA (cDNA) made from RNA isolated from the *hrl1* mutant confirmed this change. This base change altered the triplet codon to substitute a leucine (CTC) with a phenylalanine (TTC) at position 228. Leucine 228 is not a part of the active site of the enzyme but is conserved across 4-hydroxybenzoate polyprenyl diphosphate transferase (4HPT) sequences from various organisms (37). This change at a conserved position suggests the possibility of a structural change in the enzyme that may affect functionality of the enzyme.

Overexpression of HRL1 *compromises resistance against pathogens*

T-DNA insertion mutants of At4g23660 have been reported to be embryo lethal (37), and a point mutant of *HRL1* has been reported to show constitutive resistance against a variety of pathogens (11). To assess whether overexpression of *HRL1* affects resistance to pathogen, we constructed transgenic plants overexpressing the *HRL1* gene from a strong constitutive 35S promoter. Two independent transgenic lines were tested for their response to both virulent and avirulent pathogens. Rosette leaves of 4-week-old overexpression lines *HRL1 OX1*, *HRL1 OX2*, and wild-type Col-0 were infiltrated with virulent bacterial pathogens *Pst* DC3000 and *Psm* ES4326 and avirulent bacterial pathogens *Pst* DC3000 (*avrRpm1*) and *Pst* DC3000 (*avrRpt2*). Disease development and progression was monitored for 3 days post infiltration (dpi) followed by quantification of bacterial titer in leaves challenged with pathogen. *HRL1* overexpression lines developed more disease symptoms (Fig. 3A) and allowed the growth of both *Pst* DC3000 and *Psm* ES4326 virulent bacterial pathogen ~8–10-fold more than wild-type Col-0 (Fig. 3B). Similarly, *HRL1* overexpression resulted in approximately four to five-fold enhanced susceptibility against avirulent bacterial pathogens *Pst* DC3000 (*avrRpm1*) and *Pst* DC3000 (*avrRpt2*) (Fig. 3C), indicating compromised *R* gene-mediated resistance. Taken together, these results indicate a role of HRL1 in regulating the ability of plants to mount a successful defense response against bacterial pathogens.

Overexpression of HRL1 *leads to elevated Coenzyme Q_{10} levels*

HRL1 codes for 4-hydroxybenzoate polyprenyl diphosphate transferase, a key enzyme in Coenzyme Q_{10} (CoQ) biosynthesis (36, 37). Therefore, we reasoned that constitutive overexpression of *HRL1* should enhance CoQ biosynthesis, thereby leading to higher levels of CoQ in *HRL1* overexpressing plants. To measure changes in mitochondrial CoQ levels that could affect signaling, it is not enough to only quantify levels of total CoQ but it is also important to investigate the ratio of reduced/oxidized CoQ moieties, as different states of reduction of CoQ play different roles in cellular biochemistry. To determine the levels of CoQ in wild-type Col-0, *HRL1*-constitutive overexpression lines, and the *hrl1* mutant, we isolated mitochondria from these plants and assayed for total CoQ levels and their relative oxidation states. Total CoQ levels in *HRL1*-overexpression lines were found to be almost three-fold higher than in wild-type Col-0 (Supplementary Fig. S2 and Fig. 4). The *hrl1* mutant plant had half the total CoQ levels as in the wild type (Supplementary Fig. S2 and Fig. 4). In addition, we also observed a distinct shift in the ratio of ubiquinol (reduced CoQ) and ubiquinone (oxidized CoQ) moieties across different genotypes. Compared with wild-type Col-0, we observed an increase of ~10% in ubiquinone (oxidized CoQ) in *HRL1* overexpressing plants and ~5% reduction in ubiquinone (oxidized CoQ) in the *hrl1* mutant plants (Fig. 4). Taken together, these results indicate that overexpression of *HRL1* not only increases total CoQ but also shifts the balance of CoQ toward ubiquinone (oxidized CoQ), that is, away from the reduced state, therefore increasing the total available ubiquinone (oxidized CoQ) that is able to accept electrons from Complex I and/or Complex II of the mitochondrial electron transport chain. In case of the *hrl1* mutant, a shift toward lower total CoQ and lower levels of ubiquinone (oxidized CoQ) might explain observed high ROS (hydrogen peroxide and superoxide) levels in these plants due to reduced availability of electron acceptors that consequently lead to electron leakage and production of ROS (Supplementary Fig. S1B) (11).

Overexpression of HRL1 *leads to faster substrate oxidation*

To study the effect of modulation of Coenzyme Q_{10} (CoQ) levels due to overexpression and mutation of *HRL1*, we

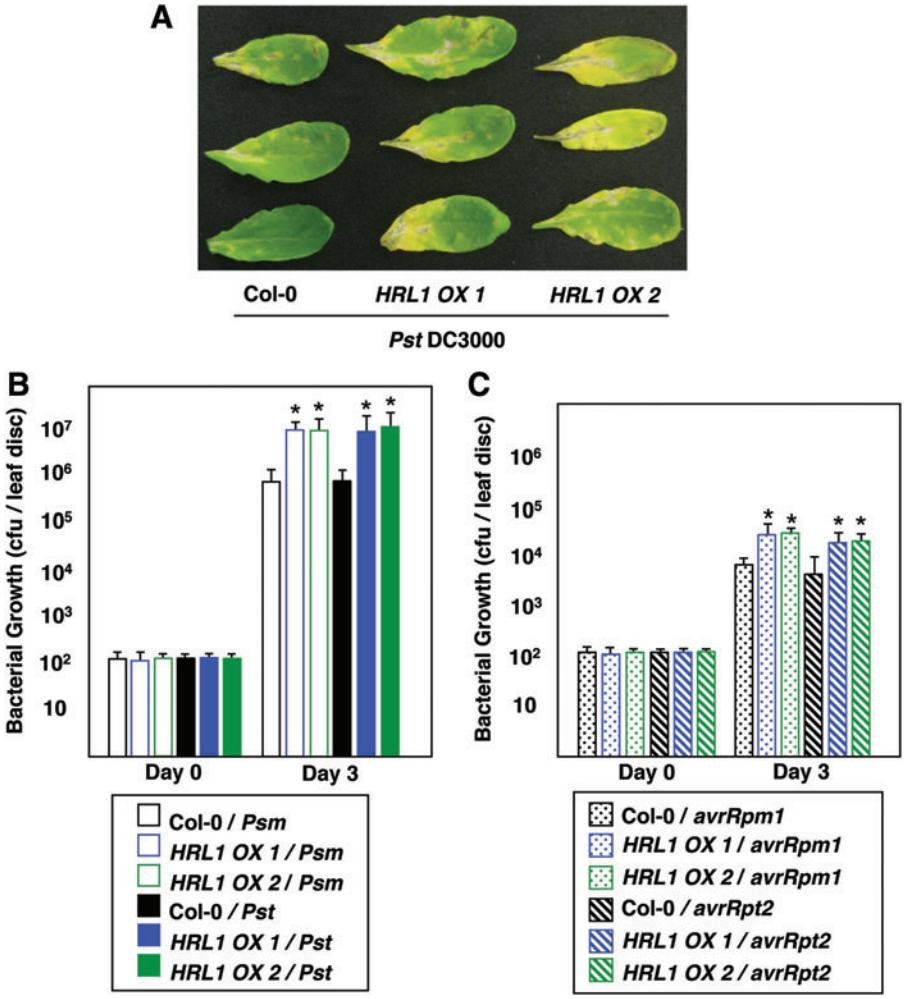

FIG. 3. ***HRL1*** **overexpression leads to compromised defense. (A)** Rosette leaves of 4-week-old plants of *HRL1* overexpressing lines and wild-type Col-0 were infiltrated with *Pst* DC3000 at a titer of 5×10^5 cfu/ml, and disease development (chlorosis- and water-soaked lesions) was monitored over a period of 5 days. Plants were photographed at 3 dpi. **(B)** Rosette leaves of 4-week-old plants were infiltrated with virulent *Psm* ES4326 (*Psm*) and *Pst* DC3000 (*Pst)* at a titer of 5×10^5 cfu/ml. For each genotype, nine plants were tested individually. Two leaf discs from each plant were collected at day 0 and 3 dpi. Bacterial growth is presented as cfu/leaf disc and represents the mean and SD of nine individual plants. The entire experiment was repeated at least twice more with plants grown at different times, and similar results were obtained. *Asterisks* indicate statistically significant differences ($*p < 0.001$, Mann–Whitney test). **(C)** Rosette leaves of 4-week-old plants were infiltrated with avirulent *Pst* DC3000 (*avrRpm1*) and *Pst* DC3000 (*avrRpt2*) at a titer of 5×10^5 cfu/ml. For each genotype, nine plants were tested individually. Two leaf discs from each plant were collected at day 0 and 3 dpi. Bacterial growth is presented as cfu/leaf disc and represents the mean and SD of nine individual plants. The entire experiment was repeated at least twice more with plants grown at different times, and similar results were obtained. *Asterisks* indicate statistically significant differences ($*p < 0.001$, Mann–Whitney test). To see this illustration in color, the reader is referred to the web version of this article at www.liebertpub.com/ars

investigated oxidative phosphorylation in the mitochondrial electron transport chain in these plants. We determined the rate of oxygen consumption (which allows estimation of rate of electron transfer) and oxidative phosphorylation in wild-type Col-0, *HRL1* overexpressing, and *hrl1* mutant plants. Succinate and ascorbate (with tetramethyl-*p*-phenylenediamine [TMPD]) were used as substrates for interrogation of mitochondrial respiratory activity (Fig. 5). Succinate was used for measuring Complex II-mediated respiration, and ascorbate (with TMPD) was used to measure Complex IV activity. Furthermore, inhibitors were used to determine the specificity of electron transfer. We observed enhanced respiration rates in the *HRL1* overexpressing plants and reduced rates in the *hrl1* mutant plants using both succinate and ascorbate (with TMPD) as substrates (Table 1 and Fig. 5). Interestingly, we hardly observed any inhibition in respiration rates in the presence of rotenone. This indicates that respiration was primarily driven by Complex II-IV activity. However, addition of antimycin A drastically reduced respiration rates when succinate was used as substrate. This points toward blockade of Complex II-mediated respiration due to inhibition of Complex III. In addition, we observed that addition of inhibitors rotenone and antimycin A did not have a significant effect on respiration rates when ascorbate (with TMPD) was used as a substrate, indicating that respiration in this case was primarily being driven by Complex IV activity. We also tested for response to

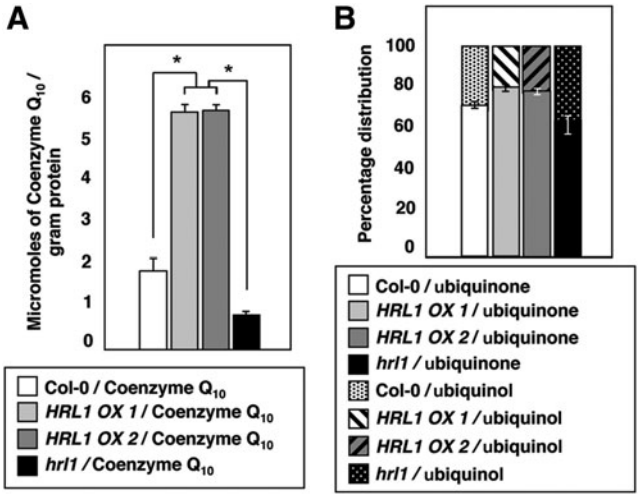

FIG. 4. HRL1 expression affects ratio of reduced/oxidized ubiquinone. (A) Total Coenzyme Q_{10} (CoQ) content in wild type (Col-0), transgenic lines (*HRL1 OX1, HRL1 OX2*), and mutant (*hrl1*) plants. *Asterisks* indicate statistically significant differences ($*p < 0.001$, Mann–Whitney test). The entire experiment was repeated at least twice more with plants grown at different times, and similar results were obtained. **(B)** Percentage distribution of ubiquinone (oxidized CoQ) and ubiquinol (reduced CoQ) in wild type (Col-0), transgenic lines overexpressing *HRL1* (*HRL1 OX1, HRL1 OX2*) and *hrl1* mutant plants.

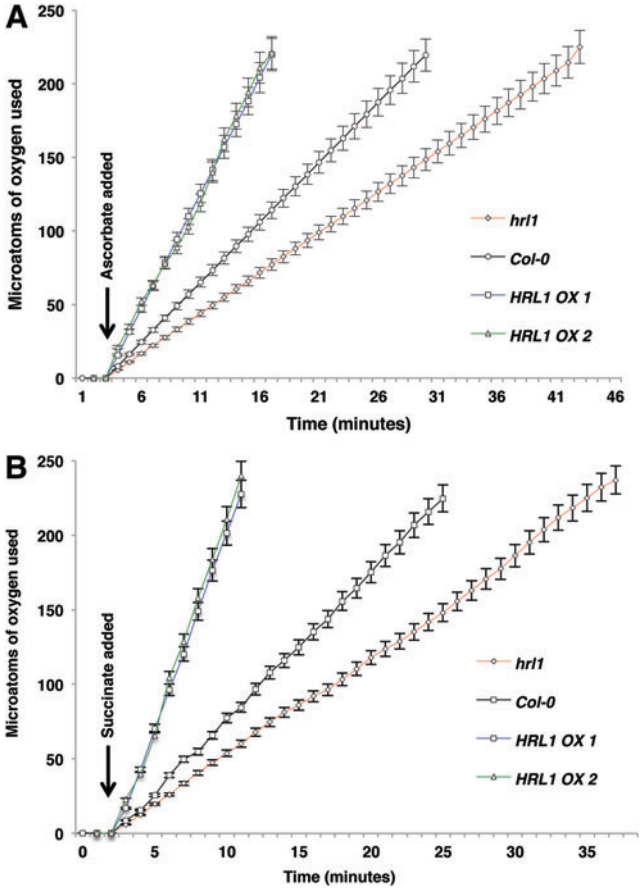

FIG. 5. Oxygen utilization by mitochondrial isolates from different genotypes. Rate of substrate oxidation in mitochondria isolated from plants of indicated genotypes. Arrow indicates time of ascorbate/TMPD **(A)**, and succinate **(B)** addition. The entire experiment was repeated at least twice more with plants grown at different times, and similar results were obtained. To see this illustration in color, the reader is referred to the web version of this article at www.liebertpub.com/ars

cyanide addition for all substrates, which resulted in severely compromised respiration, suggesting inhibition of both coupling and electron flow. Interestingly, respiration rates when using ascorbate (with TMPD), which evaluates the capacity of Complex IV, were enhanced in the *HRL1* overexpressing lines and reduced in the *hrl1* mutant. This was unexpected given that changes in levels of Coenzyme Q_{10} (CoQ) are thought to primarily affect electron flow through Complex I-III. This alteration in respiration rates may be explained due to either (a) altered flux of electrons between CoQ and cytochrome C that leads to enhanced availability of cytochrome C for ascorbate (with TMPD) or (b) an alteration in electron transport chain stoichiometry in response to changes in CoQ biosynthesis and the redox state.

Our results indicate that the rate of substrate oxidation is increased in the *HRL1* overexpression lines and reduced in the *hrl1* mutant compared with substrate oxidation in the wild-type Col-0 (Fig. 5). However, the rate of oxidative phosphorylation was unaffected in the *HRL1* overexpression and mutant lines (Table 1). This indicates that change in Coenzyme Q_{10} (CoQ) levels affected the rate of electron transfer (as is seen with change in oxygen consumption) from the electron donor to the final acceptor, oxygen, but not phosphorylation of ADP. Taken together, this indicates a possibility for reduction in the loss of electrons as a result of enhanced ubiquinone (oxidized CoQ) availability in *HRL1* overexpressing lines, resulting in reduced production of ROS.

Overexpression of HRL1 *confers resistance to high ROS environments*

To determine whether overproduction of Coenzyme Q_{10} (CoQ) in the plants overexpressing *HRL1* was affecting ROS generation *in vivo*, we exposed the plants to various high ROS environments. We reasoned that if elevated levels of CoQ due to overexpression of *HRL1* affected ROS production in a biologically relevant manner, then plants overexpressing *HRL1* should display altered responses to high ROS environments when compared with wild-type Col-0. *HRL1 OX1, HRL1 OX2*, and wild-type Col-0 seeds were plated on 1 μM paraquat (methyl viologen), 150 mM sodium chloride and exposed to 175 μM light (23 h and 15 min continuous light cycle). Paraquat is known to induce mitochondrial superoxide production at Complex I in the electron transport chain (8). Sodium chloride is well documented to induce ROS (23) *via* a variety of processes. High light stress is reported to induce high ROS levels *via* electron leakage from the photosynthetic electron transport chain (1). In all cases, *HRL1* overexpressing plants grew better than the wild-type Col-0 plants, indicating the ability of these plants to reduce the toxic effects of high ROS environments (Fig. 6). Interestingly, alternative oxidase (AOX) pathway is not affected in *HRL1* overexpressing or *hrl1* mutant plants as indicated by similar levels of ATP production (ADP/O ratios) across all genotypes (Table 1).

Table 1. Analysis of Mitochondrial Electron Transport Chain

Substrate	*Respiration rate (μatom O_2/min/mg protein)*	*ADP/O ratio*
Col-O		
Succinate	8.96 ± 0.44	1.34 ± 0.06
+ Rotenone	8.91 ± 0.39	1.36 ± 0.03
+ Antimycin A	0.23 ± 0.1	—
+ Cyanide	0.1 ± 0.0	—
Ascorbate/TMPD	7.58 ± 0.29	1.30 ± 0.05
+ Rotenone	7.54 ± 0.37	1.31 ± 0.08
+ Antimycin A	7.25 ± 0.38	1.32 ± 0.08
+ Cyanide	0.0 ± 0.0	—
hrl1		
Succinate	6.40 ± 0.31	1.36 ± 0.07
+ Rotenone	6.32 ± 0.28	1.34 ± 0.06
+ Antimycin A	0.27 ± 0.2	—
+ Cyanide	0.0 ± 0.0	—
Ascorbate/TMPD	5.35 ± 0.24	1.33 ± 0.05
+ Rotenone	5.31 ± 0.26	1.32 ± 0.03
+ Antimycin A	5.74 ± 0.28	1.34 ± 0.04
+ Cyanide	0.16 ± 0.05	—
HRL1 OX 1		
Succinate	18.69 ± 0.93	1.37 ± 0.05
+ Rotenone	18.43 ± 0.91	1.37 ± 0.03
+ Antimycin A	0.90 ± 0.1	—
+ Cyanide	0.0 ± 0.05	—
Ascorbate/TMPD	13.65 ± 0.87	1.36 ± 0.05
+ Rotenone	13.45 ± 0.88	1.35 ± 0.03
+ Antimycin A	13.32 ± 0.92	1.36 ± 0.03
+ Cyanide	0.0 ± 0.0	—
HRL1 OX 2		
Succinate	18.8 ± 0.83	1.34 ± 0.05
+ Rotenone	18.54 ± 0.86	1.36 ± 0.06
+ Antimycin A	0.84 ± 0.1	—
+ Cyanide	0.1 ± 0.0	—
Ascorbate/TMPD	13.81 ± 0.84	1.35 ± 0.08
+ Rotenone	13.69 ± 0.81	1.33 ± 0.04
+ Antimycin A	13.72 ± 0.81	1.30 ± 0.02
+ Cyanide	0.15 ± 0.0	—

Oxygen consumption and ADP/O ratios for mitochondrial isolates from indicated plants. Substrates used are succinate and ascorbate/TMPD. Inhibitors used are rotenone, antimycin A, and cyanide (Associated with Fig. 5).

In addition, *HRL1* overexpressing plants had lower levels of ROS (both hydrogen peroxide and superoxide) and did not express stress-associated molecular markers (Fig. 6B, C). This ability may be attributed to lowered metabolic ROS production in the overexpression plants, due to reduced loss of electrons as a result of enhanced ubiquinone (oxidized CoQ) availability, thereby reducing the overall ROS pool in the cell.

Discussion

The EMS-generated *hrl1* mutant of *Arabidopsis* has been characterized as an initiation lesion mimic mutant that displays spontaneous necrotic lesions, accumulates ROS, constitutively expresses defense-associated genes, accumulates higher levels of salicylic acid, and has enhanced resistance against bacterial and oomycete pathogens (11). In this study, we cloned the *HRL1* gene by positional cloning approach and found that it is predicted to code for 4-hydroxybenzoate polyprenyl diphosphate transferase (4HPT), a key enzyme that transfers the prenyl side chain to the benzoquinone frame during Coenzyme Q_{10} (CoQ) biosynthesis. CoQ serves a variety of roles in the cell ranging from its function as an electron carrier in the mitochondrial respiratory chain, in embryo development (30), in disulfide bond formation (48), and as a lipid-soluble antioxidant (17). A single base change in *hrl1*, which results in a leucine to phenylalanine substitution at a conserved residue in At4g23660, was found to result in *hrl1*-associated phenotypes. The *HRL1* (*AtPPT1)* gene has been reported to be an essential gene, because loss-of-function alleles are embryo lethal (32). These results suggest that *hrl1* is a hypomorph and partial loss of AtPPT1 function results in *hrl1*-associated phenotypes, including necrotic lesions and cell death, and the complete loss of function in *atppt1* is embryo lethal.

Overexpression of the *HRL1* gene compromises resistance against both virulent and avirulent bacterial pathogen *P. syringae.* However, resistance against virulent pathogens was compromised much more severely than against the avirulent pathogen. Basal resistance mediates defense activation against virulent pathogens (2, 18), whereas *R* gene-mediated defense activation plays a dominant role in resistance against avirulent pathogens (9). Taken together, this indicates a more important role for HRL1-mediated defense response in basal resistance as opposed to *R* gene-mediated resistance.

ROS and several signaling molecules such as nitric oxide, cyclic GMP, cyclic ADP-ribose, salicylic acid, ethylene, and jasmonic acid play a role in sensing and act as secondary messengers to initiate a resistance response (9, 10, 13, 21, 22, 29, 42). Basal resistance is defined by a single oxidative burst that is significantly less intense than the secondary oxidative burst associated with *R* gene-mediated induced defense and that builds on the primary oxidative burst.

Coenzyme Q_{10} (CoQ) biosynthesis in *Arabidopsis* is relatively well conserved. However, only a few biosynthetic enzymes have been experimentally shown to function in CoQ biosynthesis in *Arabidopsis* (37). On overexpression of the *HRL1* gene, total CoQ levels in the *HRL1* overexpression lines were significantly enhanced as compared with the wild-type Col-0. This provides further evidence in support of HRL1 being a key step of *Arabidopsis* CoQ biosynthesis. We also tested for total CoQ levels in the *hrl1* mutant and found reduced levels of total CoQ in the mutant as compared with wild-type Col-0. This indicates that the point mutation at a conserved residue in the *hrl1* mutant probably led to an inefficient enzyme, which affected CoQ biosynthesis. We also analyzed oxidative states of the total CoQ measured to ascertain ratios of oxidized and reduced CoQ, as these directly affect antioxidant abilities of CoQ. We found *HRL1* overexpressing lines and the *hrl1* mutant have enhanced and reduced levels of ubiquinone (oxidized CoQ), respectively, as compared with the wild-type Col-0. This indicates greater antioxidant ability of the *HRL1* overexpressing lines and compromised antioxidant ability of the *hrl1* mutant. An increased load of ubiquinone in *HRL1* overexpressing plants is potentially a direct effect of greater ubiquinone biosynthesis brought about by increased *4-HPT* enzyme (*AtPPT1/HRL1*) activity. This increased ubiquinone may lead to a larger CoQ

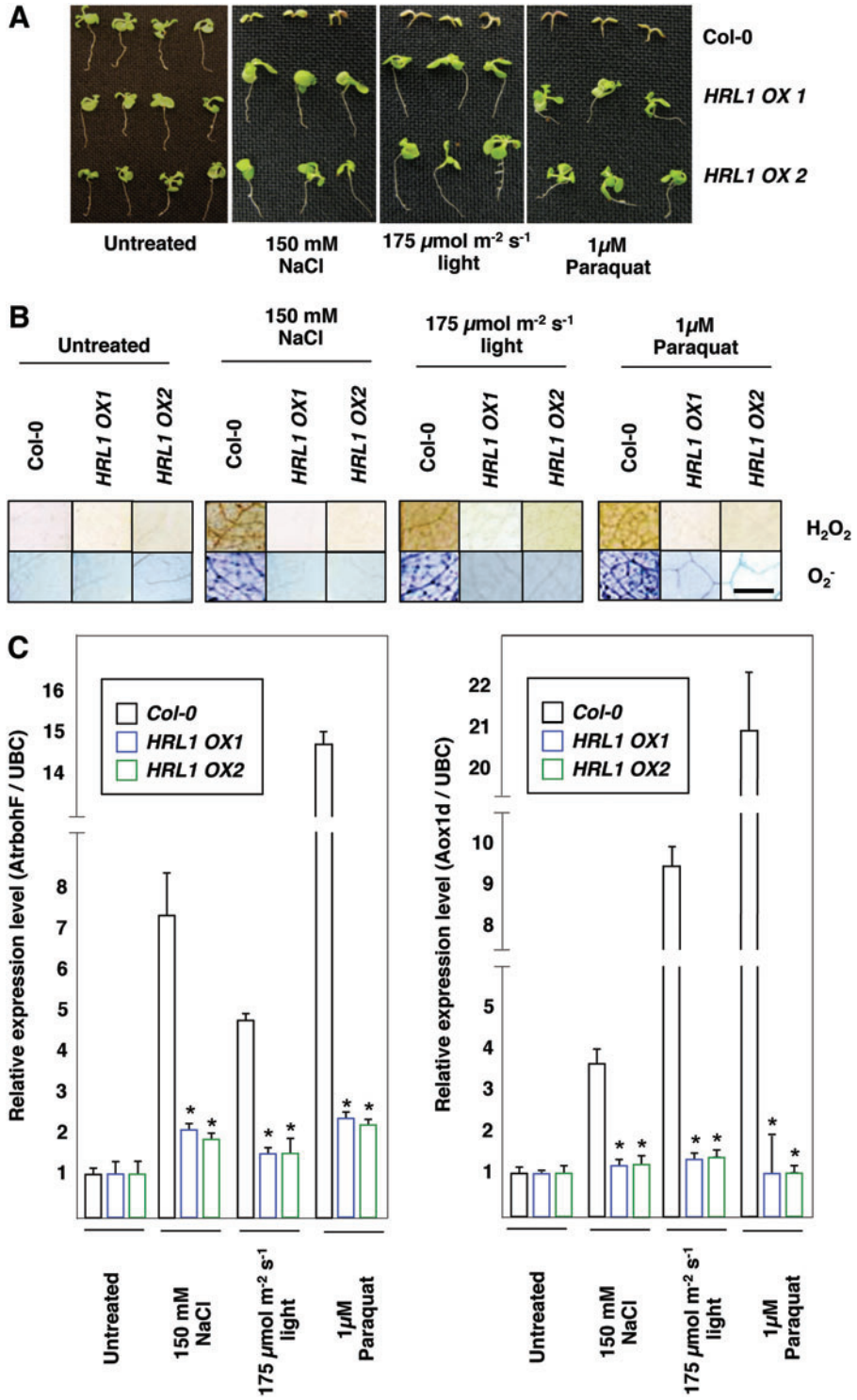

FIG. 6. *HRL1* overexpression makes plants less sensitive to reactive oxygen species (ROS). (A) Seedlings of *HRL1* overexpression lines and wild-type Col-0 were grown in normal Peters media (JR PETERS, Inc., Allentown, PA) under a 16 h light/8 h dark cycle for 14 days. Response to a high ROS environment was analyzed by transferring these seedlings to either a 23 h light/1 h dark cycle or Peters media with 150 m*M* NaCl or Peter's media with 1 μM paraquat. Seedlings were photographed after 1 week of exposure to a high ROS environment. The entire experiment was repeated at least twice more with plants grown at different times, and similar results were obtained. **(B)** Staining for hydrogen peroxide (DAB staining) and superoxide (NBT staining) levels in Col-0 and HRL1 overexpression lines under different nonbiotic stresses. Seedlings were harvested for staining after 48 h of high ROS environment. The entire experiment was repeated at least twice more, and plants grown at different times and similar results were obtained. **(C)** Gene expression analysis of *AtrbohF* and *Aox1d* by real-time PCR in Col-0 and *HRL1* overexpression lines under different abiotic stresses. Seedlings were harvested for RNA isolation after 48 h of high ROS environment. The entire experiment was repeated at least twice more with plants grown at different times, and similar results were obtained. *Asterisks* indicate statistically significant differences ($^*p < 0.001$, Mann–Whitney test). To see this illustration in color, the reader is referred to the web version of this article at www.liebertpub.com/ars

pool that alters the ubiquinol/ubiquinone ratio and, consequently, enhances the antioxidant potential. To test whether alteration in CoQ levels affected electron transport in the mitochondrial electron transport chain, we assayed for oxidative phosphorylation in the *HRL1* overexpressing lines, *hrl1* mutant, and wild-type Col-0. Both succinate and ascorbate (with TMPD) were used as substrates to examine mitochondrial respiratory activity given that they have different points of entry into the respiratory chain. In addition, inhibitors (rotenone, antimycin A, and cyanide) coupled with the substrates (succinate and ascorbate/TMPD) informed us on the mitochondrial complex specificity of electron transfer in our *HRL1* overexpressing and *hrl1* mutant plants. Our *in vitro* analysis found an increased rate of substrate oxidation in the *HRL1* overexpression lines and reduced rates in the *hrl1* mutant with no change in the rate of phosphorylation, indicating that alteration of CoQ levels affects the rate of electron transfer but not phosphorylation. Given this selective perturbation of the electron transport chain, we reasoned that the higher rate of electron transfer was facilitated

by the presence of a larger pool of ubiquinone (oxidized CoQ) available to accept electrons. This would, in turn, lead to reduction in electrons leaking out of the electron transport chain and restrict their availability toward production of ROS, thereby reducing basal ROS levels in the *HRL1* overexpression plants. Our studies using the *in vitro* system described here provide us mechanistic insights into the electron transport chain in our model. Further *in vivo* analysis using methods such as magnetic resonance spectroscopy or near-infrared spectroscopy will allow a more physiologically focused analysis.

CoQ exist in two pools—a mobile pool and a protein-bound pool that interacts with electron transport chain complexes. The two pools are in dynamic flux. The protein-bound pool is primarily responsible for transferring electrons within the respiratory complexes and the free pool functions among other things as an antioxidant reservoir. The change in electron flow seen in *HRL1* overexpressing lines and *hrl1* mutant is potentially attributable to changes in electron transport chain stoichiometry, and changes in ROS loads are probably attributable to an increase in the free pool of ubiquinone. Future investigations will interrogate electron flux changes across electron carriers and their relation to possible stoichiometric changes in the electron transport chain. In addition, we found that *HRL1* overexpressing plants are able to grow better compared with the wild-type Col-0 in environments with higher levels of ROS, indicating that lower levels of ROS in these plants may contribute to their ability to be more resistant to external sources of ROS. Interestingly, although the high ROS inducing conditions affect both the photosynthetic and mitochondrial electron transport chains, a reduction in ROS staining on *HRL1* overexpression in high ROS environments may indicate dynamic chloroplast/mitochondria crosstalk and more importantly point toward retrograde signaling as an important mediator of plant homeostasis under conditions of stress.

Taken together, our results suggest that metabolic ROS levels (due to Coenzyme Q_{10} redox states) are a significant contributor to a threshold level of basal ROS maintained due to cellular processes, which plays an important role in maintaining basal resistance against bacterial pathogens. The primary ROS burst, which is of relatively low intensity, builds on pre-existing ROS levels in the cell. Deficiency in this pre-existing ROS level further reduces the intensity of the oxidative burst and considerably affects plant response time, thereby leading to enhanced susceptibility against

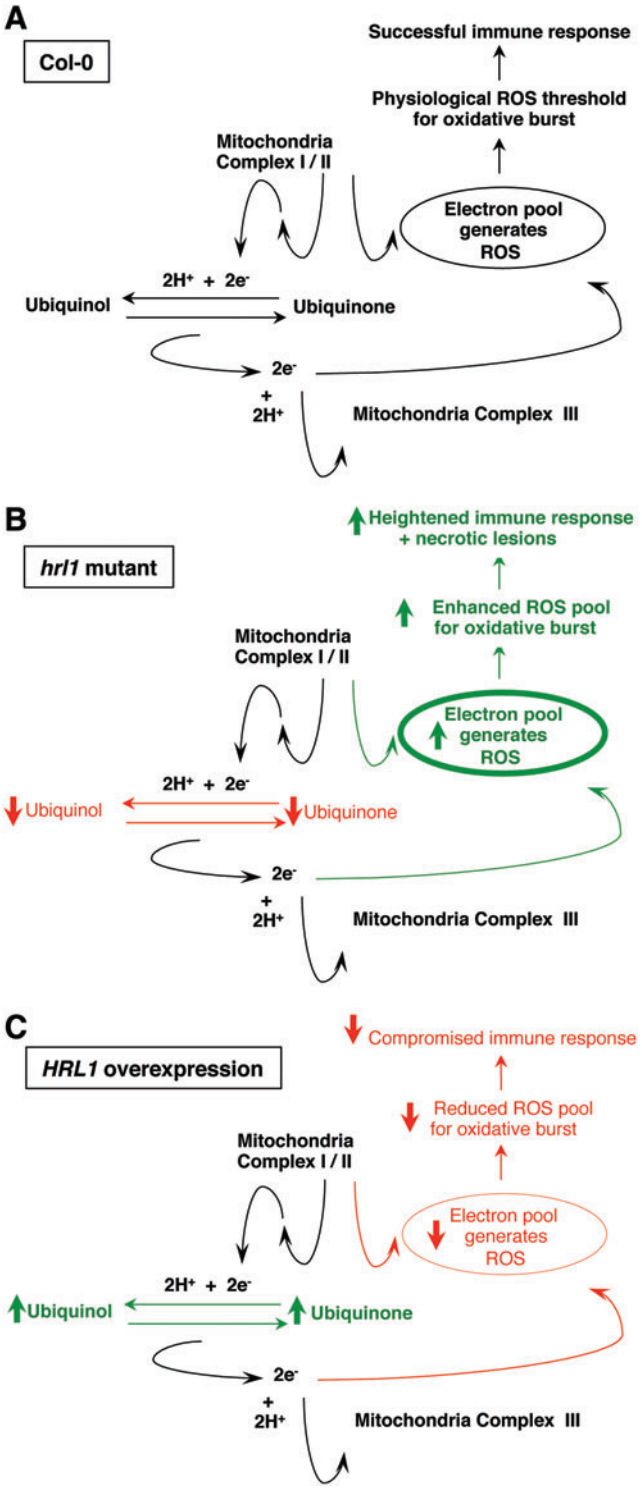

FIG. 7. Proposed model for the role of HRL1 in defense signaling. **(A)** In wild-type plants, HRL1 is involved in Coenzyme Q_{10} (CoQ) biosynthesis. CoQ acts in the mitochondrial electron transport chain (ETC) as an electron carrier by getting cyclically reduced (ubiquinol) and oxidized (ubiquinone). This electron carrier function ensures loss of minimal electrons during the oxidation/reduction process that contributes toward generation of ROS. The physiological ROS pool creates a threshold ROS level that enables effective oxidative bursts during defense against pathogens. **(B)** In *hrl1* mutants, reduced levels of CoQ compromise effective quenching of free electrons, thereby increasing electrons available for ROS production. These enhanced ROS levels contribute to activation of constitutive defense against pathogens along with a free radical-induced lesion phenotype, both of which are hallmarks of *hrl1* mutant plants. **(C)** In *HRL1* overexpression plants, increased levels of CoQ effectively quench free electrons, thereby reducing electrons available for ROS production. These reduced ROS levels lead to sub-optimal oxidative bursts required for effective defense against pathogens and thus the enhanced susceptibility against pathogens in these *HRL1* overexpressing plants. To see this illustration in color, the reader is referred to the web version of this article at www.liebertpub.com/ars

pathogen (Fig. 7). Although exact quantitation and spatial distribution of ROS is challenging, our *HRL1* overexpression and *hrl1* mutant provide us with an invaluable tool to further understand this complex signaling mechanism, especially in the context of mitochondrial retrograde signaling. It will be fascinating to quantitate the amount of ROS, the different species, and their spatial distribution to further understand the interplay that brings about basal resistance against pathogens and the ability to cope with oxidative stress environments.

Materials and Methods

Plant growth and pathogen infection of plants

Growth of bacterial pathogens, plant infections, and *in planta* pathogen growth assays were performed as previously described (11).

RNA analysis

Tissue samples were collected from soil-grown plants and were flash frozen in liquid nitrogen. Total RNA was isolated using TRIzol reagent according to the manufacturer's protocol (Invitrogen), and northern blot analysis was performed as previously described (11).

Construction and analysis of HRL1 overexpression lines

Full-length HRL1 cDNA was amplified using Platinum Taq High Fidelity DNA Polymerase (Invitrogen), forward (5′-ATGGCGTTTTTTGGGCTCTCC-3′) and reverse (5′-TTGAAAACTTCTTCCAAGTACAACTCC-3′) primers, using U16585 SSP pUNI clone (ABRC) as a template, and was cloned into pCR8/GW/TOPO TA cloning vector (Invitrogen). Sequence of the amplified product was compared with the mRNA sequences available in the public databases to confirm that the correct full-length cDNA was amplified. *HRL1* cDNA was cloned in the gateway system pMDC32 vector (ABRC) under control of a strong 35S promoter to engineer HRL1 overexpression. The construct was then introduced into wild-type Col-0 plants *via* Agrobacterium-mediated transformation (7). Transgenic plants were selected on solid Peters media supplemented with 40 μg/ml hygromycin.

Mitochondrial isolation

Isolation of fresh mitochondrial preparations for analysis was carried out essentially as described by Sweetlove *et al.* (43). Seven milligrams of *Arabidopsis* seeds were sterilized using a solution of 20% bleach and SDS. The sterilized seeds were thoroughly washed with water and grown on Peter's media. Seedlings were harvested 10 days later. All subsequent steps were performed in a cold room, and all solutions used were prechilled. Seedlings were removed from the plates, placed in a Buchner funnel, and washed with sterile distilled water. The washed seedlings were placed in a vessel and covered with 300 ml of seedling extraction medium (0.3 *M* sucrose, 25 m*M* $Na_4P_2O_7$, 2 m*M* EDTA, 10 m*M* KH_2PO_4, 1% (w/v) PVP-40, 1% (w/v) BSA, 20 m*M* ascorbic acid, pH 7.5) Tissue was homogenized and filtered through two layers of Miracloth to remove cell debris and unbroken cells. Filtrate was centrifuged for 5 min at 1100 *g*, and the resulting supernatant was collected. The supernatant was centrifuged for 20 min at 18,000 *g*, and the pellet was harvested and resuspended in 1-ml leaf mitochondria wash medium (0.3 *M* sucrose, 10 m*M* TES-KOH, pH 7.5). Centrifugation at 18,000 *g* and resuspension in 1 ml leaf mitochondria wash medium was repeated to obtain an organelle suspension. The organelle suspension was layered onto the surface of two 28% Percoll, 0%–4.4% PVP-40 gradients. Density-gradient centrifugation was carried out at 40,000 *g* for 40 min. Mitochondria formed a white/pale brown band toward the bottom of the gradient. The mitochondrial band was transferred to a fresh tube and resuspended in 20 ml leaf mitochondria wash medium followed by centrifugation at 31,000 *g* for 15 min. The pellet is harvested, re-suspended in 20 ml leaf mitochondria wash medium, and recentrifuged. Finally, this was followed by resuspension of the mitochondrial pellet in 0.5 ml leaf mitochondria wash medium.

Coenzyme Q_{10} quantitation

Estimation of CoQ and analysis of oxidative phosphorylation was performed as described by Redfearn and Pumphrey (39, 41, 49). Twenty milligrams of mitochondrial protein was denatured by addition of cold methanol containing 1 mg/ml pyrogallol (which protects ubiquinol from oxidation) followed by addition of 5 ml of light petroleum. The mixture was vortexed and then centrifuged for 3 min to separate different layers. The upper light petroleum layer was transferred to another tube, and the extraction was repeated. The light petroleum extract was treated with 2 ml of 95% (v/v) methanol and mixed gently. The mixture was exposed to a vacuum desiccator to evaporate the solvent. The residual lipid was dissolved in 3 ml of spectroscopically pure ethanol, and the spectrum was determined between 230 and 320 nm. To reduce the ubiquinone to ubiquinol, 0.2 mg of sodium borohydride was added to the mix and spectrum was redetermined at the same wavelength range. Absorbance at 275 nm was used to determine ubiquinone amount in samples tested.

Measurement of substrate oxidation and oxidative phosphorylation

Estimation of CoQ and analysis of oxidative phosphorylation was performed as described by Redfearn and Pumphrey (39, 41, 49). Fresh mitochondrial suspension solutions were mixed with assay medium containing 17.5 m*M* K_2HPO_4, 50 m*M* Tris-HCl, 0.4 *M* sucrose, 75 m*M* KCl, 1 mM EDTA, 5 m*M* $MgCl_2$, and 3 mg BSA. The mixture was enclosed in a constantly stirred cuvette. Oxygen uptake was measured polarographically using a Clark electrode coupled to a Perkin-Elmer recorder (4, 5, 38). Freshly isolated mitochondrial samples (to maintain phosphorylation activity) were mixed in a buffer solution containing bovine serum albumin (BSA) (to avoid mitochondrial uncoupling of oxidative phosphorylation due to traces of fatty acids) and ascorbate/TMPD or succinate (as an electron donor). The reaction was carried out in a temperature-controlled cuvette, and utilization of oxygen was recorded as a function of time. The reaction was further spiked with ADP, and similar recordings were made to determine the rate for oxidative phosphorylation. Finally, inhibitors (rotenone, antimycin A, and cyanide) were added to the reaction to ascertain that oxygen utilization being recorded was due to the mitochondrial electron transport chain and was not an artifact of the experimental conditions.

ROS sensitivity assays

Wild-type Col-0 and *HRL1* overexpression seeds were sterilized and plated on Peter's media with 1 μM paraquat and 150 mM sodium chloride. For high light conditions, seeds were exposed to 175 μM of constant light in 23:15 h cycles. Germination and growth were monitored till 3 weeks.

Histochemistry and microscopy

Staining for the presence of hydrogen peroxide was done by the DAB method as previously described (11). Staining for superoxide was done using NBT staining method as previously described (11).

Real-time PCR

Tissue samples were collected from Peters media plate grown plants after 48 h and were flash frozen in liquid nitrogen. Plants were grown under indicated conditions. Total RNA was isolated using TRIzol reagent according to the manufacturer's protocol (Invitrogen). cDNA was prepared according to the manufacturer's protocol (Invitrogen). Real-time qPCR analysis was performed using a Bio-Rad Real-Time PCR detection system. Gene expression analysis of *AtrbohF* and *Aox1d* was performed, and changes in expression levels were computed using the $2^{-\Delta\Delta Ct}$ method (31)

Acknowledgments

The authors thank Dr. Barbara Kunkel for various *P. syringae* strains, Arabidopsis Biological Resource Center (ABRC) for CS60000 seeds, binary vector pYLTAC7, pMDC32 vector, and U16585 SSP pUNI clone. This work was supported in part by a grant from the National Science Foundation (NSF) (IBN-0313492) and funds from Syracuse University to RR.

Author Disclosure Statement

No competing financial interests exist.

References

1. Asada K. Production and scavenging of reactive oxygen species in chloroplasts and their functions. *Plant Physiol* 141: 391–396, 2006.
2. Belkhadir Y, Subramaniam R, and Dangl JL. Plant disease resistance protein signaling: NBS-LRR proteins and their partners. *Curr Opin Plant Biol* 7: 391–399, 2004.
3. Bradley DJ, Kjellbom P, and Lamb CJ. Elicitor- and wound-induced oxidative cross-linking of a proline-rich plant cell wall protein: a novel, rapid defense response. *Cell* 70: 21–30, 1992.
4. Braidot E, Petrussa E, Vianello A, and Macri F. Hydrogen peroxide generation by higher plant mitochondria oxidizing complex I or complex II substrates. *FEBS Lett* 451: 347–350, 1999.
5. Chance B and Williams GR. The respiratory chain and oxidative phosphorylation. *Adv Enzymol Relat Subj Biochem* 17: 65–134, 1956.
6. Chen SX and Schopfer P. Hydroxyl-radical production in physiological reactions. A novel function of peroxidase. *Eur J Biochem* 260: 726–735, 1999.
7. Clough SJ and Bent AF. Floral dip: a simplified method for Agrobacterium-mediated transformation of *Arabidopsis thaliana*. *Plant J* 16: 735–743, 1998.
8. Cocheme HM and Murphy MP. Complex I is the major site of mitochondrial superoxide production by paraquat. *J Biol Chem* 283: 1786–1798, 2008.
9. Dangl JL and Jones JD. Plant pathogens and integrated defence responses to infection. *Nature* 411: 826–833, 2001.
10. Delledonne M, Polverari A, and Murgia I. The functions of nitric oxide-mediated signaling and changes in gene expression during the hypersensitive response. *Antioxid Redox Signal* 5: 33–41, 2003.
11. Devadas SK, Enyedi A, and Raina R. The *Arabidopsis hrl1* mutation reveals novel overlapping roles for salicylic acid, jasmonic acid and ethylene signalling in cell death and defence against pathogens. *Plant J* 30: 467–480, 2002.
12. Doke N, Miura Y, Sanchez LM, Park HJ, Noritake T, Yoshioka H, and Kawakita K. The oxidative burst protects plants against pathogen attack: mechanism and role as an emergency signal for plant bio-defence—a review. *Gene* 179: 45–51, 1996.
13. Durner J, Wendehenne D, and Klessig DF. Defense gene induction in tobacco by nitric oxide, cyclic GMP, and cyclic ADP-ribose. *Proc Natl Acad Sci U S A* 95: 10328–10333, 1998.
14. Felix G, Duran JD, Volko S, and Boller T. Plants have a sensitive perception system for the most conserved domain of bacterial flagellin. *Plant J* 18: 265–276, 1999.
15. Fester T and Hause G. Accumulation of reactive oxygen species in arbuscular mycorrhizal roots. *Mycorrhiza* 15: 373–379, 2005.
16. Frederickson Matika DE and Loake G. Redox regulation in plant immune function. *Antioxid Redox Signal* 21: 1373–1388, 2013.
17. Frei B, Kim MC, and Ames BN. Ubiquinol-10 is an effective lipid-soluble antioxidant at physiological concentrations. *Proc Natl Acad Sci U S A* 87: 4879–4883, 1990.
18. Glazebrook J, Rogers EE, and Ausubel FM. Use of *Arabidopsis* for genetic dissection of plant defense responses. *Annu Rev Genet* 31: 547–569, 1997.
19. Gleason C, Huang S, Thatcher LF, Foley RC, Anderson CR, Carroll AJ, Millar AH, and Singh KB. Mitochondrial complex II has a key role in mitochondrial-derived reactive oxygen species influence on plant stress gene regulation and defense. *Proc Natl Acad Sci U S A* 108: 10768–10773, 2011.
20. Grant JJ, Yun BW, and Loake GJ. Oxidative burst and cognate redox signalling reported by luciferase imaging: identification of a signal network that functions independently of ethylene, SA and Me-JA but is dependent on MAPKK activity. *Plant J* 24: 569–582, 2000.
21. Hammond-Kosack KE and Parker JE. Deciphering plant-pathogen communication: fresh perspectives for molecular resistance breeding. *Curr Opin Biotechnol* 14: 177–193, 2003.
22. Han Y, Chaouch S, Mhamdi A, Queval G, Zechmann B, and Noctor G. Functional analysis of *Arabidopsis* mutants points to novel roles for glutathione in coupling H(2)O(2) to activation of salicylic acid accumulation and signaling. *Antioxid Redox Signal* 18: 2106–2121, 2013.
23. Hasegawa PM, Bressan RA, Zhu JK, and Bohnert HJ. Plant Cellular and Molecular Responses to High Salinity. *Annu Rev Plant Physiol Plant Mol Biol* 51: 463–499, 2000.
24. Jones JD and Dangl JL. The plant immune system. *Nature* 444: 323–329, 2006.
25. Kaku H, Nishizawa Y, Ishii-Minami N, Akimoto-Tomiyama C, Dohmae N, Takio K, Minami E, and Shibuya N. Plant cells recognize chitin fragments for defense signaling

through a plasma membrane receptor. *Proc Natl Acad Sci U S A* 103: 11086–11091, 2006.
26. Konieczny A and Ausubel FM. A procedure for mapping *Arabidopsis* mutations using co-dominant ecotype-specific PCR-based markers. *Plant J* 4: 403–410, 1993.
27. Kovtun Y, Chiu WL, Tena G, and Sheen J. Functional analysis of oxidative stress-activated mitogen-activated protein kinase cascade in plants. *Proc Natl Acad Sci U S A* 97: 2940–2945, 2000.
28. Lamb C and Dixon RA. The Oxidative Burst in Plant Disease Resistance. *Annu Rev Plant Physiol Plant Mol Biol* 48: 251–275, 1997.
29. Laxalt AM and Munnik T. Phospholipid signalling in plant defence. *Curr Opin Plant Biol* 5: 332–338, 2002.
30. Levavasseur F, Miyadera H, Sirois J, Tremblay ML, Kita K, Shoubridge E, and Hekimi S. Ubiquinone is necessary for mouse embryonic development but is not essential for mitochondrial respiration. *J Biol Chem* 276: 46160–46164, 2001.
31. Livak KJ and Schmittgen TD. Analysis of relative gene expression data using real-time quantitative PCR and the 2(-Delta Delta C(T)) Method. *Methods* 25: 402–408, 2001.
32. Melillo MT, Leonetti P, Bongiovanni M, Castagnone-Sereno P, and Bleve-Zacheo T. Modulation of reactive oxygen species activities and H2O2 accumulation during compatible and incompatible tomato-root-knot nematode interactions. *New Phytol* 170: 501–512, 2006.
33. Mittler R, Vanderauwera S, Suzuki N, Miller G, Tognetti VB, Vandepoele K, Gollery M, Shulaev V, and Van Breusegem F. ROS signaling: the new wave? *Trends Plant Sci* 16: 300–309, 2011.
34. Moller IM. Plant mitochondria and oxidative stress: electron transport, NADPH turnover, and metabolism of reactive oxygen species. *Annu Rev Plant Physiol Plant Mol Biol* 52: 561–591, 2001.
35. Mur LA, Kenton P, Lloyd AJ, Ougham H, and Prats E. The hypersensitive response; the centenary is upon us but how much do we know? *J Exp Bot* 59: 501–520, 2008.
36. Ohara K, Yamamoto K, Hamamoto M, Sasaki K, and Yazaki K. Functional characterization of OsPPT1, which encodes p-hydroxybenzoate polyprenyltransferase involved in ubiquinone biosynthesis in Oryza sativa. *Plant Cell Physiol* 47: 581–590, 2006.
37. Okada K, Ohara K, Yazaki K, Nozaki K, Uchida N, Kawamukai M, Nojiri H, and Yamane H. The AtPPT1 gene encoding 4-hydroxybenzoate polyprenyl diphosphate transferase in ubiquinone biosynthesis is required for embryo development in *Arabidopsis thaliana*. *Plant Mol Biol* 55: 567–577, 2004.
38. Racker E. *Membranes of Mitochondria and Chloroplasts.* New York: Van Nostrand Reinhold Co., 1970. pp. xiii, 322.
39. Redfearn ER and Pumphrey AM. The kinetics of ubiquinone reactions in heart-muscle preparations. *Biochem J* 76: 64–71, 1960.
40. Robson CA and Vanlerberghe GC. Transgenic plant cells lacking mitochondrial alternative oxidase have increased susceptibility to mitochondria-dependent and -independent pathways of programmed cell death. *Plant Physiol* 129: 1908–1920, 2002.
41. Salabei JK, Gibb AA, and Hill BG. Comprehensive measurement of respiratory activity in permeabilized cells using extracellular flux analysis. *Nat Protoc* 9: 421–438, 2014.
42. Skelly MJ and Loake GJ. Synthesis of redox-active molecules and their signaling functions during the expression of plant disease resistance. *Antioxid Redox Signal* 19: 990–997, 2013.
43. Sweetlove LJ, Taylor NL, and Leaver CJ. Isolation of intact, functional mitochondria from the model plant *Arabidopsis thaliana*. *Methods Mol Biol* 372: 125–136, 2007.
44. Thoma I, Loeffler C, Sinha AK, Gupta M, Krischke M, Steffan B, Roitsch T, and Mueller MJ. Cyclopentenone isoprostanes induced by reactive oxygen species trigger defense gene activation and phytoalexin accumulation in plants. *Plant J* 34: 363–375, 2003.
45. Torres MA, Jones JD, and Dangl JL. Reactive oxygen species signaling in response to pathogens. *Plant Physiol* 141: 373–378, 2006.
46. Tripathy BC and Oelmuller R. Reactive oxygen species generation and signaling in plants. *Plant Signal Behav* 7: 1621–1633, 2012.
47. Vanlerberghe GC, Robson CA, and Yip JY. Induction of mitochondrial alternative oxidase in response to a cell signal pathway down-regulating the cytochrome pathway prevents programmed cell death. *Plant Physiol* 129: 1829–1842, 2002.
48. Xie T, Yu L, Bader MW, Bardwell JC, and Yu CA. Identification of the ubiquinone-binding domain in the disulfide catalyst disulfide bond protein B. *J Biol Chem* 277: 1649–1652, 2002.
49. Zhang J, Nuebel E, Wisidagama DR, Setoguchi K, Hong JS, Van Horn CM, Imam SS, Vergnes L, Malone CS, Koehler CM, and Teitell MA. Measuring energy metabolism in cultured cells, including human pluripotent stem cells and differentiated cells. *Nat Protoc* 7: 1068–1085, 2012.

Address correspondence to:
Dr. Ramesh Raina
Department of Biology
Syracuse University
Syracuse, NY 13244

E-mail: raraina@syr.edu

Date of first submission to ARS Central, April 20, 2014; date of final revised submission, December 15, 2014; date of acceptance, January 1, 2015.

Abbreviations Used

4HPT = 4-hydroxybenzoate polyprenyl diphosphate transferase
ABRC = Arabidopsis Biological Resource Center
AtPPT1 = *Arabidopsis thaliana* polyprenyltransferase 1
BAC = bacterial artificial chromosome
BSA = bovine serum albumin
cfu = colony forming unit
Col-0 = Columbia
CoQ = Coenzyme Q_{10}
dpi = day post infiltration
EMS = ethyl methanesulfonate
ETI = effector triggered immunity
HR = hypersensitive response
hrl1 = hypersensitive response-like lesions 1
L*er* = Landsberg *erecta*
PAMP = pathogen-associated molecular pattern
PTI = PAMP-triggered immunity
R-gene = resistance gene
ROS = reactive oxygen species
TMPD = tetramethyl-*p*-phenylenediamine